

Silicate species of water glass and insights for alkali-activated green cement

Helén Jansson,^{1,a} Diana Bernin,^{2,b} and Kerstin Ramser^{3,c}

¹Department of Civil and Environmental Engineering, Chalmers University of Technology, SE-41296 Gothenburg, Sweden

²Swedish NMR Centre, Gothenburg University, Gothenburg, 41390 Sweden

³Department of Engineering Sciences and Mathematics, Luleå University of Technology, 971 87 Luleå, Sweden

(Received 7 May 2015; accepted 16 June 2015; published online 29 June 2015)

Despite that sodium silicate solutions of high pH are commonly used in industrial applications, most investigations are focused on low to medium values of pH. Therefore we have investigated such solutions in a broad modulus range and up to high pH values (~ 14) by use of infrared (IR) spectroscopy and silicon nuclear magnetic resonance ($^{29}\text{Si-NMR}$). The results show that the modulus dependent pH value leads to more or less charged species, which affects the configurations of the silicate units. This in turn, influences the alkali-activation process of low CO_2 footprint cements, i.e. materials based on industrial waste or by-products. © 2015 Author(s). All article content, except where otherwise noted, is licensed under a Creative Commons Attribution 3.0 Unported License. [<http://dx.doi.org/10.1063/1.4923371>]

I. INTRODUCTION

Sodium silicate solutions ($\text{Na}_2\text{O}\cdot n\text{SiO}_3$), commonly also called water glass, are among the most widely used chemicals in industrial products. For instance, water glass is commonly used as binders or adhesives in various applications, to increase the fire and acid resistance in materials, as detergents or to enhance the strength of cements and concretes.¹ In addition, different water glass compositions are frequently used for the alkali-activation of green, i.e. low CO_2 footprint, cementitious mineral materials.² As shown in the literature, this type of solutions has a complex molecular structure and phase behavior, see e.g.,³⁻⁷ which is highly dependent on pH.³ Despite of years of investigations, there are still questions about the molecular species configuration of these solutions that need to be answered to gain clarity over the best conditions for the various applications such as those mentioned above. In particular, for higher pH values the structure and behavior of this type of solutions are not well established.³

When adding sodium hydroxide (NaOH) to a water glass, the ratio (molar or weight) $\text{SiO}_2/\text{Na}_2\text{O}$ is decreased. This ratio is called water glass modulus (n) and determines various physical and chemical properties such as the pH and the viscosity of the solution. For instance, a previous study⁸ on water glass showed that the viscosity is extremely dependent on the modulus and increases as the solution becomes either more siliceous or more alkaline, i.e. at both higher and lower $\text{SiO}_2/\text{Na}_2\text{O}$ molar ratios (n). Since the viscosity of such disperse systems like this is given by the silicate conformation i.e. extended chain conformation and the degree of polymerization, it was suggested⁸ that increasing or decreasing the moduli, from the point of the minimum value of the viscosity, results in that either larger or smaller aggregates of silicate anions dominates in the solution.

Recently it was found that the alkali-activation of the green cementitious material ground granulated blastfurnace slag (GGBS) is highly dependent on the modulus (n) of the water glass, and

^aCorresponding author: helen.jansson@chalmers.se, Phone: +46 31 772 3297, Fax: +46 31 772 1993

^bdiana.bernin@nrmr.gu.se

^ckerstin.ramser@ltu.se



that the initial setting time shows a V-formed trend.⁹ A very similar modulus dependence was also observed previously for initial setting time of another type of alkali-activated green cements.¹⁰ In both studies,^{9,10} the shortest initial setting time of the water glass activated material was obtained for modulus $n = 2$, whereas both lower and higher moduli resulted in longer initial setting times. Interestingly, the initial setting time of alkali-activated cementitious materials follows the same behavior as the viscosity of the water glass; the initial setting time has a minimum close to the value of minimum in viscosity of the solutions.⁸ Other studies indicate that the early reaction of alkali-activated mineral materials is diffusion controlled,^{11,12} and therefore also dependent on the viscosity of the initial mixture.¹³ Furthermore, it has been shown that the initial state of the gelation process of alkali-activated mineral materials is dependent on the degree of polymerization of the predominant silicate species in the alkali-solution.¹⁴ Taken this into account, it might be essential to explore the modulus dependent changes of these liquids in order to reach a fundamental understanding of the initial setting time behavior and hydration process of alkali-activation of cementitious mineral materials.

In order to get a fundamental understanding of various silicate unit configurations as a function of moduli we applied infrared spectroscopy (IR) and silicon nuclear magnetic resonance (²⁹Si-NMR), which monitors bond vibrations and the main configurations of the silicate units in the solution, respectively. Although the focus of this study is on the modulus dependent structure of water glass, the outcome will give insight to the effect of different moduli (n) of water glass on the initial setting time of green cement, i.e. to the point at which the material loses its plasticity during the initial stage of the hydration. However, since water glass of high pH values are frequently used in various industrial the findings are widely applicable.

II. EXPERIMENTAL

This study focuses on exploring the silicate configurations of water glass of various moduli ranging from $n = 0.99$ - 3.35 . As the starting solution, a commercial available water glass from Sibelco Nordic, which contains 27.6 wt% SiO₂ and modulus $n = 3.35$, was used. The modulus n of this water glass was varied by the addition of NaOH solutions of different concentrations (previously prepared by dissolving appropriate amounts of sodium hydroxide pellets (Fisher Scientific) in deionized water). Each solution was prepared more than one day prior to the measurements in order to allow for thermal equilibrium. Characteristics of the investigated water glass solutions are shown in table I.

One dimensional (1D) Silicon nuclear magnetic resonance (²⁹Si-NMR) experiments were performed on an 11.7 T Varian Inova spectrometer operating at a ²⁹Si resonance frequency of 99.39 MHz at 24 °C. The magnet was equipped with a broadband probe containing glass. For each measurement, glass NMR tubes were filled with roughly 600 µl water glass solution. To reduce any background contribution from the probe and the glass tube a RIDE¹⁵⁻¹⁷ pulse sequence was used. The spectra were acquired using a spectral width of 19800 Hz, an acquisition time of 0.5 s and 9900 points. The recycle delay was 10 s. The signal prior to a Fourier transform was accumulated for 4096 scans. For comparison, the spectra were normalized by the SiO₂ concentration.

Infrared (IR) spectra were collected by using a Bruker IR spectrometer. Each spectrum was taken in reflectance mode with 500 scans in the wavenumber interval 600 – 7500 cm⁻¹. Before the measurements, a background spectrum was taken that was automatically subtracted from the

TABLE I. pH values of the water glass solutions of various moduli n .

Modulus (molar) n	pH
3.35	11.2
2.59	11.8
2.07	12.6
1.69	13.3
0.99	13.9

measured spectra. A number of consecutive preprocessing steps were applied to the raw spectra. Smoothing was employed using Eilers' algorithm with $d = 2$ and $\lambda = 10$.¹⁸ The spectral background was subtracted by fitting a piecewise polynomial to each spectrum.¹⁹ The spectra were vector normalized so that the integrated intensities were equalized for a quantitative comparison of the results. The analysis of the peaks in the Si-region (from about 800 – 1200 cm^{-1}) was performed by curve fitting the spectra by Gaussians functions.

The initial setting time of a ground granulated blastfurnace slag (GGBS) called Merit 5000 (SSAB Merox AB) was measured as a function of modulus n of the water glass used for the alkali activation by use of a Vicat instrument (Toni Technik) equipped with a calibrated weight of 300 g and a cylindrical needle with a flat tip area of 1 mm^2 . A schematic illustration of the method is shown in the right panel of figure 1.

III. RESULTS

A. Initial setting time of alkali-activated ground granulated blastfurnace slag (GGBS)

The hydration process of GGBS starts with the so-called dissolution phase in which GGBS particles are gradually dissolved and released ions diffuse out from the particle surface into the surrounding liquid. Subsequently, the ions in the solution phase react and form so-called hydration products, which nucleate on the particle surfaces. At a certain point the particles become bound together in clusters, a network is formed throughout the material and the material changes from a viscous liquid like slurry, in which particles are dissolved, to an interconnected more solid like phase. In analogy with the hydration process of ordinary cements,²⁰ this point can be considered as a solid percolation threshold, i.e. the material loses its plasticity, and the penetration of the Vicat needle (see inset of figure 1) is prevented to a specific degree. This is the so-called initial setting time.

In figure 1, the measured initial setting times for the GGBS are shown, as a function of water glass modulus n , of the solution used for the alkali activation. As can be observed from this figure, the initial setting time is the fastest for the water glass of modulus $n = 2.07$ and becomes slower at both higher and lower moduli.

B. ²⁹Si Nuclear magnetic resonance (NMR) on water glass

The normalized ²⁹Si-NMR spectra (see figure 2) show different peak patterns for various water glass compositions (moduli). Harris et al.²¹ assigned peaks close to -80 ppm to cyclic Q^2 species (see figure 2) because of smaller Si-O-Si bond angles compared to linear Q^2 units, which are located

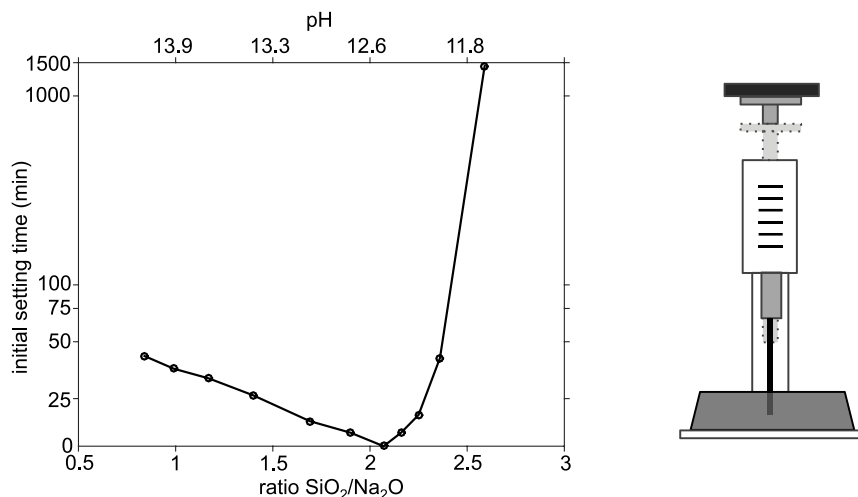


FIG. 1. Initial setting time as a function of water glass modulus n ($\text{SiO}_2/\text{Na}_2\text{O}$ ratio) for alkali activated ground granulated blastfurnace slag (GGBS) and a schematic illustration of the Vicat method.

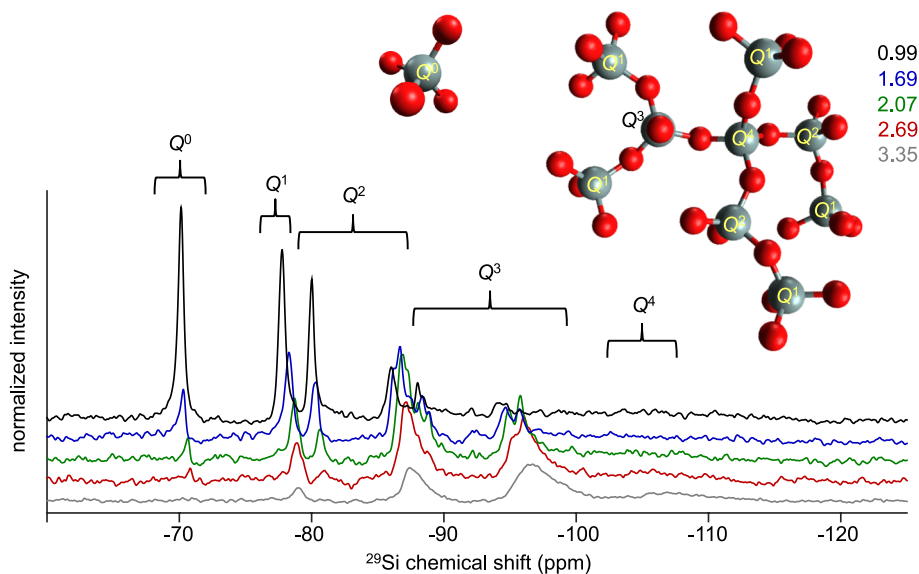


FIG. 2. Normalized ^{29}Si -NMR spectra for water glass of moduli $n = 3.35 - 0.99$ and a schematic illustration of the silicate configurations Q^0 to Q^4 . Assignments of the peaks are according to Ref. 22.

around -88 ppm.^{5,22} The same is true for the Q^3 groups. For the initial water glass solution with a modulus $n = 3.35$ (i.e. the lowest sodium content) the spectrum shows broad peaks, which are assigned to larger aggregates, containing $Q^1 - Q^3$ whereas more simple silicate anions (Q^0 units) are completely absent. For this composition there is also a weak indication of the highly connected Q^4 configuration.

By reducing the modulus, the broad peaks start to split into multiple narrower peaks and indicate the presence of e.g. a distribution of different aggregates containing Q^3 configurations. For lower moduli, the ^{29}Si spectra reveal also Q^0 peaks arising from the silicate anion. Our results are in agreement with earlier studies, see e.g. Refs. 21 and 22 that reported on depolymerization of silicates with increasing sodium content. Furthermore, a decrease in modulus and thus an increase in pH shifts the peak position to higher ppm values, which is attributed to deprotonation of Si-OH groups or silicate-sodium ion pairing.²² It should be noted that by use of the RIDE sequence in liquid state ^{29}Si -NMR only a qualitative distribution of various building groups and silicate structures can be obtained.

C. Infrared spectroscopy (IR) on water glass

From IR spectroscopy, figure 3, it is obvious that there are significant differences between the different compositions both in the water stretching and bending vibrations. All spectra reveal a broad peak with center around 3250 cm^{-1} which is due to hydrogen bonded OH groups. In this broad peak there is a shoulder around 3500 cm^{-1} , which can be assigned to symmetric (ν_1) and asymmetric (ν_3) stretching vibrations of OH. Around 1600 cm^{-1} the scissoring bend (ν_2) of H_2O can be seen. For the OH-vibrations it can, for instance, be observed that the intensity of the very broad band with a center at 3250 cm^{-1} is changed for different moduli. The intensity initially increases and the maximum intensity is found for the sample with $n = 2.59$. However, for the highest modulus, $n = 3.35$, the intensity around 3250 cm^{-1} decreases to the same value as for the lowest modulus at $n = 0.99$. As also can be observed from figure 3, the main peak around 1000 cm^{-1} in the silicate fingerprint region ($800 - 1200\text{ cm}^{-1}$) is shifted to higher wavenumbers as the modulus is increased (i.e. when the sodium content is decreased). The highest and lowest wavenumbers of this peak is thus found for the highest and lowest modulus, respectively.

However, the actual silicate structure of the water glass solutions cannot be obtained from figure 3. To distinguish the contribution of different structural units a curve fitting procedure was

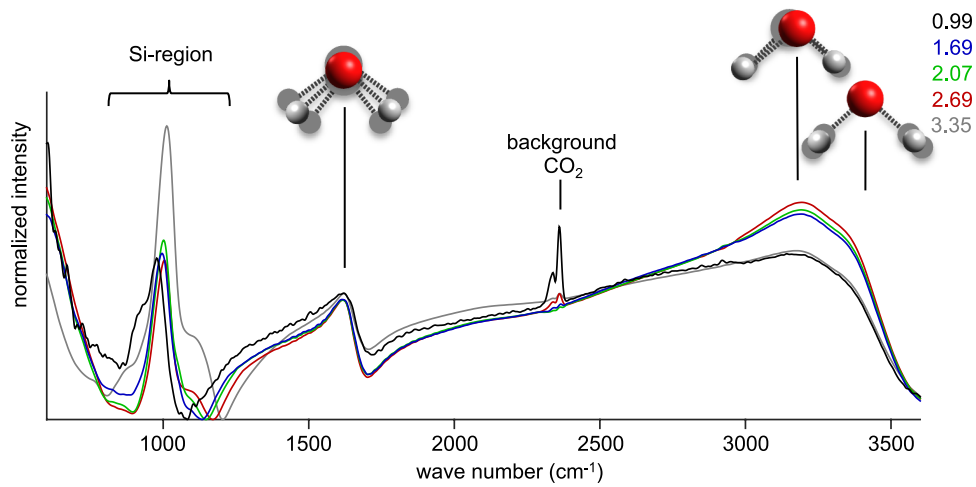


FIG. 3. Normalized Infrared spectra for water glass of moduli $n = 3.35-0.99$ with schematic representations of stretching (peak centered around 3250 cm^{-1}) and bending (1600 cm^{-1}) of OH groups. The silicate fingerprint region is found between 800 and 1200 cm^{-1} .

performed. The result is shown in figure 4. In the histogram in figure 4, seen below right hand side, the differences between the different peaks are shown in terms of percent fractions. As can be observed, the spectra obtained for all water glass of higher moduli are similar, whereas the solution of the lowest modulus differs ($n = 0.99$) substantially. For the solution of higher moduli, the spectra can be fitted by five Gaussian functions with peak maxima (denoted 1-5) at approximately 850 , 964 ± 6 , 1007 ± 7 , 1060 ± 10 and $1098 \pm 15 \text{ cm}^{-1}$, where the most dominant peak is located around 1007 cm^{-1} . For the water glass solution of the lowest modulus $n = 0.99$ there was a need for 6 Gaussians (denoted 1-6) to fit the silicate region of the spectrum.

IV. DISCUSSION

A. ^{29}Si Nuclear magnetic resonance (NMR) on water glass

The degree of polymerization of silicate anions in water glass is dependent on the silicate and sodium ions concentrations, the modulus and the pH, see e.g.³⁻⁵ The different units are often

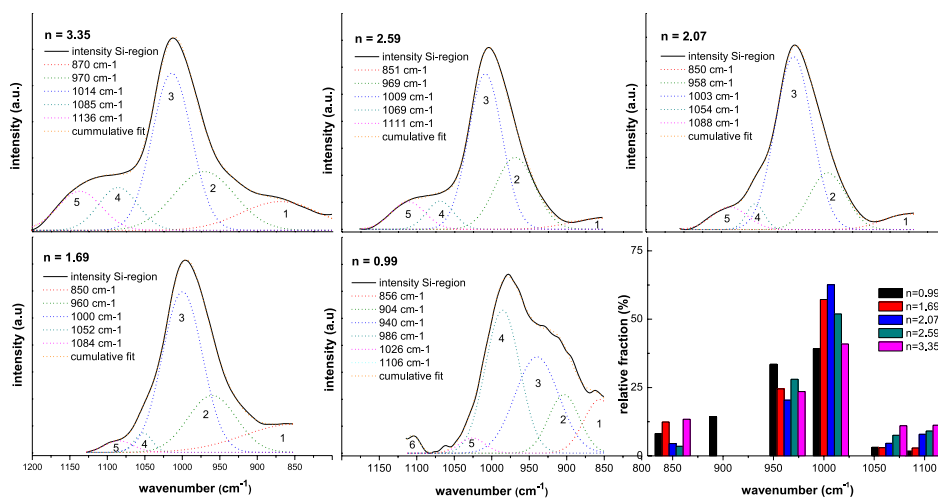


FIG. 4. Spectral deconvolution (curve fitting) of IR spectra acquired of the silicate region as a function of modulus. Histogram at the right-hand side below, shows the percent fractions of the different peaks.

denoted by the NMR nomenclature for the silicate connectivity called Q^X . In this terminology, X ranges from 0-4 and denotes the number of neighboring Si atom(s) connected to a SiO_4^{4-} tetrahedron via the oxygen atom. However, in water glass, the dissolved silicate anions (SiO_4^{4-}) can be protonated, interact with sodium ions or take part in the polymerization of larger aggregates, which are composed of $Q^1 - Q^4$ configurations. A schematic illustration of the different connectivities is shown in figure 2. In solutions different types of aggregates such as monomers, dimers, trimers and combinations of them generally coexist^{4-6,23} which form linear, branched or cyclic structures.⁵ It should be noted that the largest silicate configuration Q^4 is only expected to be found in highly connected and branched configurations^{6,7} and should therefore be absent in diluted solutions.

With ²⁹Si-NMR it is possible to distinguish between various silicate connectivities. As seen in the result section, the NMR spectra (figure 2) show that the silicate configuration differs for the water glass of different moduli. The highest modulus ($n = 3.35$) gives rise to broad peaks, which indicates larger aggregates while Q^0 units seem to be absent. When the modulus is decreased, the broad NMR bands start to split up due to the splitting of the aggregates into smaller ones. The shift in peak position to larger ppm values results from an increase in pH (i.e. decrease in modulus), which forms more negatively charged Si-O⁻ groups that can interact with the positively charged sodium ions. For the water glass of modulus $n = 3.35$ there is an indication of a Q^4 configuration, which could arise from the NMR glass tube or the glassy part of the probe. However, since we used the RIDE pulse sequence¹⁵⁻¹⁷ and since there is no indication of any Q^4 configuration in the spectra obtained for the solutions of lower modulus, this should not be the case.

B. Infrared spectroscopy (IR) on water glass solutions

The intensity behavior in the water stretching and bending vibrations around 3250 and 1600 cm^{-1} implies that more water molecules (OH-groups) contribute to the vibration at the intermediate concentrations of sodium. The increasing intensity with increasing moduli is in accordance with a previous study where it was found that the quasi free OH groups decrease with increasing salt concentration, since more anions in the solutions lead to more and stronger docking sites for OH groups.^{24,25} However, for the highest moduli $n = 3.35$, the abrupt decrease of the ν_1 and the ν_3 peak in the spectrum could be explained by the binding of OH to the large silicate aggregates, as seen in the ²⁹Si-NMR. The addition of ions to water leads to a decrease of the symmetric and asymmetric stretch character of the tetrahedral hydrogen-bonded network, and thus to a decrease of the 3250 cm^{-1} peak intensity.

As mentioned above, modification of the modulus n and pH creates various silicate configurations,³⁻⁵ affecting the viscosity of the solutions⁸ and also the gelation process of cementitious mineral materials¹⁴ in which the reaction between silicates and dissolved calcium ions from alkali-activated mineral materials are involved. Therefore, we will here concentrate on the silicate region located in the interval 800-1200 cm^{-1} . Note that it is evident that the relative intensity, the shape and the extension of the region varies with the modulus n (figure 3).

From previous IR studies on water glass⁴ (and references therein) it has been suggested that larger silicate structures contributes to the IR spectrum at higher wavenumbers and small molecular weight units at lower wavenumber, respectively. Hence, both the extension of the silicate region to particularly larger wavenumbers and the shift of the main peak (around 1000 cm^{-1}) indicate that the size of the structural units increases with increasing modulus, which is in agreement with the results obtained by ²⁹Si-NMR.

The curve fitting procedure (figure 4) showed that spectra of water glass of higher moduli are similar while the one with the lowest modulus differs substantially, i.e. the numbers of Gaussians necessary for the curve fitting increased from 5 to 6. As shown in figure 4, for the latter most of the peaks are found at somewhat different positions compared to the water glass of higher moduli, which should indicate that the molecular structure is substantially changed. It can also be noted that a new peak appears at about 904 cm^{-1} and that the main peak is centered at about 986 cm^{-1} . The latter suggests that the smallest silicate structural units are found in this concentration, which is also confirmed by the ²⁹Si NMR measurements shown above. Even if the present study is focused on the structure of water glass, it can be noted that the main peak around 1000 cm^{-1} is interesting

also when studying the structure and structure development of calcium-silicate-hydrate (CSH) gel of alkali-activated slag and the degree of polymerization in geopolymerization, respectively.^{26–28} In general, the intensity of this peak increases and the peak maximum is moving to higher wavenumbers when the structure becomes more polymerized; i.e. when larger structures are developed.

However, although often used in the literature, recent studies^{7,29} on water glass made of dissolved sodium metasilicates have shown that the generally used NMR terminology regarding silicate connectivity and configuration most likely cannot be used directly for describing specific IR vibrations of water glasses. Instead it was suggested that for such solutions of higher pH ($\text{pH} > 10$), the observed IR vibrations in the silicate region are dependent on the sodium ion content and due to various degrees of dissociation of sodium ions. According to these studies,^{7,29} the shift towards lower wavenumbers with decreased moduli implies that more sodium ions are interacting with the oxygen atoms on the silicate tetrahedrons. This is also what is obtained for the here investigated samples where the position of the most intense peak if moved from 1015 cm^{-1} for the water glass of lowest sodium content ($n = 3.35$) to 985 cm^{-1} for the sample of highest sodium content ($n = 0.99$). When the peak maximum comes close to 985 cm^{-1} , as for the $n = 0.99$ sample, the specific configuration bonds giving rise to this peak is a neutral silicate structure where all oxygen atoms on the silicate tetrahedron are protonated or occupied by sodium ions.^{7,29} In the histogram in figure 4 it can be observed that for $n = 2.07$ the main peak around 1000 cm^{-1} displays a maximum and the peak at 964 cm^{-1} shows a minimum when compared to the other moduli. This latter peak is, according to Halasz et al.,^{7,29} due to Si-OH vibrations. Interestingly, this solution gives rise to the fastest setting time as shown in our previous study⁹ (see figure 1).

C. Silicate configuration and insights for the alkali-activation of green cementitious materials

According to the ²⁹Si spectra, the solution with modulus $n = 3.35$ is dominated by larger silicate aggregates, which suggests that a large amounts of the sodium ions in the material are incorporated, or buried, in the silicate structures. As a consequence, only a few sites of negatively charged oxygens on the silica aggregates should be available for interaction with, for instance, dissolved ions in the surrounding. As the modulus n is decreased, larger silicate structural units break up and become smaller and thereby also a larger fraction of oxygen sites are found on the corners of the silicate aggregates.

With increased modulus n , the pH of the water glass is increased, which in turn influences the solubility of ions.³⁰ An increased pH results in reduced solubility of calcium ions whereas the opposite is found for silicates.^{30,31} This should have an effect on the initial stage, the so-called dissolution phase, of the hydration process of alkali-activated green cementitious materials like GGBS. In the dissolution phase GGBS bonds are broken, and ions like calcium ions migrate out of the slag material into the liquid phase surrounding the GGBS particles.³² However as can be observed from figure 1, despite that the solubility of calcium ions is reduced, the smaller size of the structural silicate units results in an increased (faster) initial setting time of GGBS. The reason for this is most likely that the probability for interaction between dissolved ions and negatively charged oxygen sites on the silicate aggregates increases.

The fastest initial setting time of water glass activated GGBS was previously found to occur for modulus close to 2, both by us⁹ (see figure 1) and others.¹⁰ It is also close to the water glass composition for which a minimum in the viscosity is observed.⁸ Thus, even if the solubility of calcium ions is further decreased due to increased pH ($\text{pH} = 12.6$), the alkali-activated mixture (i.e. GGBS and water glass) becomes more fluid due to the smaller size of the silicate aggregates. Consequently, the diffusion process, important for the reaction and structure development of the alkali-activated slag,¹¹ is facilitated.

As shown in figure 1, the initial setting time becomes longer when the alkali solution becomes either more siliceous or more alkaline (i.e. higher or lower moduli). With further decrease of modulus, the position of the main peak in the infrared spectrum is moved to lower wavenumber, which indicates that less negatively charged corners appear at the silicate structures. In addition, the

results from the ^{29}Si NMR measurements indicate that the silicate aggregates get more depolymerized. At the same time the solubility of calcium ions from the slag is decreased due to the increase in pH.³⁰ Thus, only a small amount of dissolved calcium ions will be available for the pozzolanic reaction at the same time as the fraction of negatively charged sites are lower and, as expected, the initial setting time becomes longer as can be seen in figure 1.

For the solution of the lowest modulus ($n = 0.99$) larger silicate aggregates are completely absent and the solution consists to a large extent only of smaller structural units like Q^0 and Q^1 . At this water glass composition the pH is close to 14 and the total amount of sodium ions in the solution are high (see table I). However as mentioned above, previous studies^{7,29} have shown that when the peak position of the main peak is located around 985 cm^{-1} , most oxygen sites on the silicate tetrahedrons are occupied by either hydrogen or sodium ions. Thus, in this case fewer amounts of negatively charged oxygen sites are available for dissolved calcium ions, and as a result, the initial setting time is further increased.

V. CONCLUSIONS

By using a combination of ^{29}Si -NMR, and IR we have revealed that for higher and lower moduli (lower and higher sodium content, respectively) the structural units of silicate species in the water glass solution vary. Larger silicate units are found in water glass of higher modulus. As the modulus is decreased, these larger structures are split up into smaller aggregates, which results in changes of the viscosity of the solutions. The silicate structures are stabilized by electrostatic interactions between oxygen atoms on the corners of the silicate tetrahedrons and sodium ions, respectively. The fastest initial setting time of GGBS is found when using water glass of modulus 2.07 for alkali activation. This implies an excess of charged sites (O^-) on the silicate structures that ions can interact which is favorable for the initial setting time of GGBS or other types of reactions.

ACKNOWLEDGEMENT

The Swedish research council FORMAS and the Climate KIC project Building Technologies Acceleration are acknowledged for financial support. Also acknowledged are Prof Mattias Grahn and PhD Elisaveta Potapova at Luleå University of Technology for assistance with the IR spectrometer, and The Swedish NMR Centre for spectrometer time.

¹ *Ullmann's encyclopedia of industrial chemistry*, 7th ed. (John Wiley and Sons, Inc, 2000).

² C. Shi, P. V. Krivenko, and D. Roy, *Alkali-activated cement and concretes* (Taylor and Frances Group, London and New York, 2006).

³ J. Nordstrom, E. Nilsson, P. Jarvol, M. Nayeri, A. Palmqvist, J. Bergenholtz, and A. Matic, "Concentration- and pH-dependence of highly alkaline sodium silicate solutions," *J. Colloid Interface Sci.* **356**(1), 37-45 (2011).

⁴ D. Dimas, I. Giannopoulou, and D. Panias, "Polymerization in sodium silicate solutions: a fundamental process in geopolymerization technology," *J. Mater. Sci.* **44**(14), 3719-3730 (2009).

⁵ G. Engelhardt and D. Michel, *High resolution solid state NMR of silicates and zeolites* (John Wiley & Sons, Australia, 1987).

⁶ G. Engelhardt, D. Zeigan, H. Jancke, D. Hoebbel, and W. Wieker, " ^{29}Si NMR-spectroscopy of silicate solutions 2. Dependence of structure of silicate anions in water solutions from Na-Si ratio," *Z. Anorg. Allg. Chem.* **418**(1), 17-28 (1975).

⁷ I. Halasz, M. Agarwal, R. Li, and N. Miller, "What can vibrational spectroscopy tell about the structure of dissolved sodium silicates?," *Microporous Mesoporous Mater.* **135**(1-3), 74-81 (2010).

⁸ X. Yang, W. Zhu, and Q. Yang, "The viscosity properties of sodium silicate solutions," *J. Solution Chem.* **37**(1), 73-83 (2008).

⁹ H. Jansson and L. Tang, "The initial setting time of ground granulated blastfurnace slag GGBS and its relation to the modulus of the alkali-activating solution," in *Proceeding of the XXII Nordic Concrete Research Symposium (NCR), Reykjavik, Iceland*, (2014).

¹⁰ S. A. Bernal, J. L. Provis, V. Rose, and R. Mejia de Gutierrez, "Evolution of binder structure in sodium silicate-activated slag-metakaolin blends," *Cem. Concr. Compos.* **33**(1), 46-54 (2011).

¹¹ A. FernandezJimenez and F. Puertas, "Alkali-activated slag cements: Kinetic studies," *Cem. Concr. Res.* **27**(3), 359-368 (1997).

¹² D. Ravikumar and N. Neithalath, "Reaction kinetics in sodium silicate powder and liquid activated slag binders evaluated using isothermal calorimetry," *Thermochim. Acta* **546**, 32-43 (2012).

¹³ T. W. Cheng and J. P. Chiu, "Fire-resistant geopolymer produced by granulated blast furnace slag," *Miner. Eng.* **16**(3), 205-210 (2003).

- ¹⁴ M. Criado, A. Fernandez-Jimenez, A. Palomo, I. Sobrados, and J. Sanz, "Effect of the SiO₂/Na₂O ratio on the alkali activation of fly ash. Part II: ²⁹Si MAS-NMR Survey," *Microporous Mesoporous Mater.* **109**(1-3), 525-534 (2008).
- ¹⁵ W. Kozminski and K. Jackowski, "Application of adiabatic inversion pulses for elimination of baseline distortions in Fourier transform NMR. A natural abundance ¹⁷O NMR spectrum for gaseous acetone," *Magn. Reson. Chem.* **38**(6), 459-462 (2000).
- ¹⁶ J. Schraml, P. Sandor, S. Korec, M. Krump, and B. Foller, "Improved baseline in ²⁹Si NMR spectra of water glasses," *Magn. Reson. Chem.* **51**(7), 403-406 (2013).
- ¹⁷ K. Woelk, P. Trautner, H. G. Niessen, and R. E. Gerald, "RIDE' n RIPT-ring down elimination in rapid imaging pulse trains," *J. Magn. Reson.* **159**(2), 207-212 (2002).
- ¹⁸ P. H. C. Eilers, "A perfect smoother," *Anal. Chem.* **75**(14), 3631-3636 (2003).
- ¹⁹ A. Cao, A. K. Pandya, G. K. Serhatkulu, R. E. Weber, H. Dai, J. S. Thakur, V. M. Naik, R. Naik, G. W. Auner, R. Rabah, and D. C. Freeman, "A robust method for automated background subtraction of tissue fluorescence," *J. Raman Spectrosc.* **38**(9), 1199-1205 (2007).
- ²⁰ J. Zhang, E. A. Weissinger, S. Peethamparan, and G. W. Scherer, "Early hydration and setting of oil well cement," *Cem. Concr. Res.* **40**(7), 1023-1033 (2010).
- ²¹ R. K. Harris and C. T. G. Knight, "²⁹Si NMR-studies of aqueous silicate solutions 4. Tetraalkylammonium hydroxide solutions," *J. Mol. Struct.* **78**(3-4), 273-278 (1982).
- ²² S. D. Kinrade and T. W. Swaddle, "²⁹Si NMR-studies of aqueous silicate solutions 1. Chemical shifts and equilibria," *Inorg. Chem.* **27**(23), 4253-4259 (1988).
- ²³ R. O. Gould, B. M. Lowe, and N. A. Macgillp, "Investigation of aqueous sodium metasilicate solutions by ²⁹Si NMR-spectroscopy," *Journal of the Chemical Society-Chemical Communications* (17), 720-721 (1974).
- ²⁴ L. M. Levering, "A vibrational spectroscopic study of aqueous hydrogen halide solutions: Application to atmospheric aerosol chemistry," Thesis, The Ohio State University, 2005, https://research.chemistry.ohio-state.edu/allen/files/2011/09/thesis_levering_ms_3_05.pdf.
- ²⁵ J. Riemenschneider, "Spectroscopic investigations on pure water and aqueous salt solutions in the mid infrared region," Thesis, University of Rostock, 2011, http://rosdok.uni-rostock.de/file/rosdok_disshab_0000000812/rosdok_derivate_0000004838/Dissertation_Riemenschneider_2012.pdf.
- ²⁶ I. Lecomte, C. Henrist, M. Liegeois, F. Maseri, A. Rulmont, and R. Cloots, "(Micro)-structural comparison between geopolymers, alkali-activated slag cement and Portland cement," *J. Eur. Ceram. Soc.* **26**(16), 3789-3797 (2006).
- ²⁷ F. Puertas and A. Fernandez-Jimenez, "Mineralogical and microstructural characterisation of alkali-activated fly ash/slag pastes," *Cem. Concr. Compos.* **25**(3), 287-292 (2003).
- ²⁸ P. Chindapasirt, C. Jaturapitakkul, W. Chalee, and U. Rattanasak, "Comparative study on the characteristics of fly ash and bottom ash geopolymers," *Waste Manage. (Oxford)* **29**(2), 539-543 (2009).
- ²⁹ I. Halasz, M. Agarwal, R. Li, and N. Miller, "Vibrational spectra and dissociation of aqueous Na₂SiO₃ solutions," *Catal. Lett.* **117**(1-2), 34-42 (2007).
- ³⁰ S. S. Zumdahl, *Chemical principles*, 4th ed. (2002).
- ³¹ S. J. Song and H. M. Jennings, "Pore solution chemistry of alkali-activated ground granulated blast-furnace slag," *Cem. Concr. Res.* **29**(2), 159-170 (1999).
- ³² A. R. Brough and A. Atkinson, "Sodium silicate-based, alkali-activated slag mortars Part I. Strength, hydration and microstructure," *Cem. Concr. Res.* **32**(6), 865-879 (2002).